

# Time evolution and morphological characteristics of white light flare on 18 January 1989

J.Y. Xuan<sup>2</sup>, X.M. Gu<sup>1,2</sup>, J. Lin<sup>2</sup>, Y.C. Jiang<sup>2</sup>, S.H. Zhong<sup>2</sup>, and Y.S. Li<sup>2</sup>

<sup>1</sup> CCAST (World Laboratory), P.O. Box 8730, Beijing 100080, China

<sup>2</sup> Yunnan Observatory, P.O. Box 110, Kunming 650011, China

Received May 30, 1995; accepted September 4, 1997

**Abstract.** Some properties of the white light flare (WLF) that occurred on 18 January 1989 are presented. The flare consisted of 7 patched-shape kernels, with sizes  $(1.5 \sim 4) 10^{17} \text{ cm}^2$ . The lifetimes of the kernels were from several minutes to more than 40 minutes. The initial bright points of the WLF kernels originated between the umbra and penumbra, in penumbra fibrils, between penumbra fibrils and the photosphere, or on the photosphere and light bridge. These kernels appeared 2 to 3 minutes after  $H\alpha$  flares, and reached their maxima respectively before the first maximum and 1 to 2 minutes before the second maximum of the  $H\alpha$  flare, and disappeared slowly before the disappearance of the  $H\alpha$  flare. The direction and size of material motion in the kernels are different. The precursors of the WLF are similar to those of ordinary flares. The magnetic pattern of the photosphere in the active region is in  $\delta$ -structure, and the kernels lie at or near the changing magnetic neutral lines. The small longitudinal field gradient may be constrained by the small transverse field on the photosphere. The flare exhibited both temporal and spatial properties in the center reversal and line-width of  $H\alpha$  profiles, and has characteristics of both class I and II. Thus it may be a mixed-class white light flare.

**Key words:** sun: flares

## 1. Introduction

Solar white light flares (WLFs) are a class of flares that can be observed in the optical continuum (Fang & Ding 1994), and seem to have no difference from ordinary flares except for the optical continuum. However, the energy emitted in the continuum is much higher than that in spectral lines, nearly 90% of the total emission energy. Therefore, WLFs are considered as an extreme case of flares. It is generally considered that the initial energy release in flares takes place in the corona. However, the continuum emission of WLFs comes mainly from the lower

chromosphere and photosphere. It is difficult to interpret the phenomenon with the traditional theory of flare radiative transfer and atmospheric model (Neidig 1989).

86 WLFs had been observed from 1 September 1859 to 1992, according to the statistical results by Neidig & Cliver (1983a), Xuan et al. (1991), Sakurai et al. (1992), Neidig et al. (1993) and Schmieder et al. (1994). Later, 7 WLFs were identified from the data of solar flares (see Table 1). It is possible that some WLFs have not yet been identified, and more will be found with new analysis. Machado et al. (1985), and Fang & Ding (1994) divided those WLFs into two classes according to the shape and the intensity of  $H\alpha$  lines in the Balmer series (see Table 2). Most of the WLFs are in class I, and only 6 in class II. Physical mechanisms and origins may be different for these two types of WLFs (Fang & Ding 1994). Therefore, further study is necessary on properties and origins of WLFs.

The multi-band optical observations of the white light flare on 18 January 1989 with the Spectrograph SSHG of Yunnan Observatory (Xuan et al. 1991) are important and valuable in understanding the evolution of WLFs and their morphological characteristics.

## 2. Observations

On 18 January 1989, solar activity in the active region AR 5312 enhanced obviously from 05:00 to 09:52UT, and ordinary flares appeared one after another (NOAA 1989). The active region was monitored with the multi-band optical instrument (see Table 4) at Yunnan Observatory.

### 2.1. Observations

A series of  $H\alpha$  filtergrams of the active region was obtained with the vacuum solar telescope (Instrument 1, Wu et al. 1990) from 03:30 to 08:18UT on 18 January (see Table 3 and Fig. 1). The data of scanning photographs and synchronous  $H\alpha$  filtergrams of the white light flare (S30 W65) were also obtained with the two-dimension multi-band spectroheliograph SSHG (Instrument 2, Xuan

**Table 1.** Some more WLFs supplemented by 1994

Date	Type	Beg.	Max.	End	Position	Imp.	Datum type
09/26/63 <sup>(1)</sup>	H $\alpha$ WLF		07:21 07:16		N15W75	-/-	Sp <sup>a</sup>
11/10/74 <sup>(2)</sup>	H $\alpha$ WLF		03:31		N12E02	1N/-	Sp
09/19/79 <sup>(2)</sup>	H $\alpha$ WLF		23:08 23:02		N06E33	3B/X5	Sp
12/30/82 <sup>(3)</sup>	H $\alpha$ WLF		01:49		S13W22	1N/M7	Sp
05/09/83 <sup>(2)</sup>	H $\alpha$ WLF		23:11		S30E40	2B/X2	MB <sup>b</sup>
06/06/91 <sup>(4)</sup>	H $\alpha$ WLF	00:58 01:05	01:08	04:31 01:06	N33E44	4B/X12	MB
10/28/91 <sup>(5)</sup>	H $\alpha$ WLF	07:37E	07:43U 07:37	07:47D	S15E04	SN/M1.5	†

<sup>a</sup> spectral data, <sup>b</sup> filtergrams in multi-bands and <sup>c</sup> H $\alpha$  filtergrams.

(1) Sotirovski et al. (1992), (2) Fang & Ding (1994), (3) Huang et al. (1991)

(4) Zhu & Shen (1992)

(5) Yunnan Observatory, † Sighted in WL by naked eyes.

**Table 2.** Classifications and corresponding behaviours of WLFs

Class I	Class II
Shows significant temporal relationships between maximum of WLF continuous emissions and those of hard X-ray and radio bursts	No such relationships observed
Strong Balmer jump in spectra may be observed	No Balmer jump shows
Emissions of Balmer lines are strong and wide	Emissions of Balmer lines are weak and narrow
The center reversal of H $\alpha$ emission line is significant	

& Lin 1993) in three wave bands (H $\alpha$ , H $\beta$  and H $\gamma$ ) during five different time intervals from 07:00UT to 07:52UT (Xuan et al. 1991). In the meantime, fine structure observations (see Figs. 2 and 3) of sunspots in the region were made with the solar photosphere telescope (Instrument 3, see Table 4) of Yunnan Observatory several days before and after 18 January. The longitudinal components of the magnetic field during the same time interval were also obtained with the solar magnetic field telescope (Ai & Hu 1986) at the Huairou Station of Beijing Observatory (see Fig. 3).

## 2.2. Data processing

The lifetime of the WLF and sizes of the kernels before maximum (see Table 5) were obtained by comparing the spectral data with H $\alpha$  filtergrams. The spectral films were measured with a PDS microdensitometer and processed

on a VAX-8350 computer. The changes of the spectral line profiles in the WLF kernels are shown in Fig. 4 (see Sect. 3.3).

## 3. Characteristics of the flare kernels

On 18 January, vigorous activity appeared in the active region AR 5312, and flare evolution, characteristics and related conditions can be seen obviously in the multi-band optical data. It is shown from Tables 3 and 5 and Figs. 1 and 2 that activities of ordinary (or H $\alpha$ ) flares took place frequently and kernels of the WLF were brightening continuously.

### 3.1. The sources of kernels and their motions

The original bright points of kernels 1 (containing 4 smaller bright points), 4 and 5 (from an ordinary flare) were located between umbra and penumbra of sunspots or in penumbra fibrils. After the bright points became brighter and larger, they covered the umbra and penumbra of the sunspots or photosphere. The original bright points of kernels 2 (containing 4 smaller bright points), 3, 6 (containing 3 smaller bright points) and 7 were located on the plages lying respectively in penumbra of sunspots, on the photosphere or at two ends of the extended light bridge connecting sunspots  $B_1$  and  $B_2$ . The penumbra of sunspots, photosphere or plages were covered by the brightening and enlarged bright points.

The H $\alpha$  off-band observations (see the bottom of Fig. 1) show that before and after the first maximum of the ordinary flares the redshift was stronger than the blue shift. However, kernel 3 showed blue shift in 3 intervals before and after the maximum of the WLF. For kernel 6, before, during and after the maximum of the WLF, its leading part (in the west limb) changed from blue to

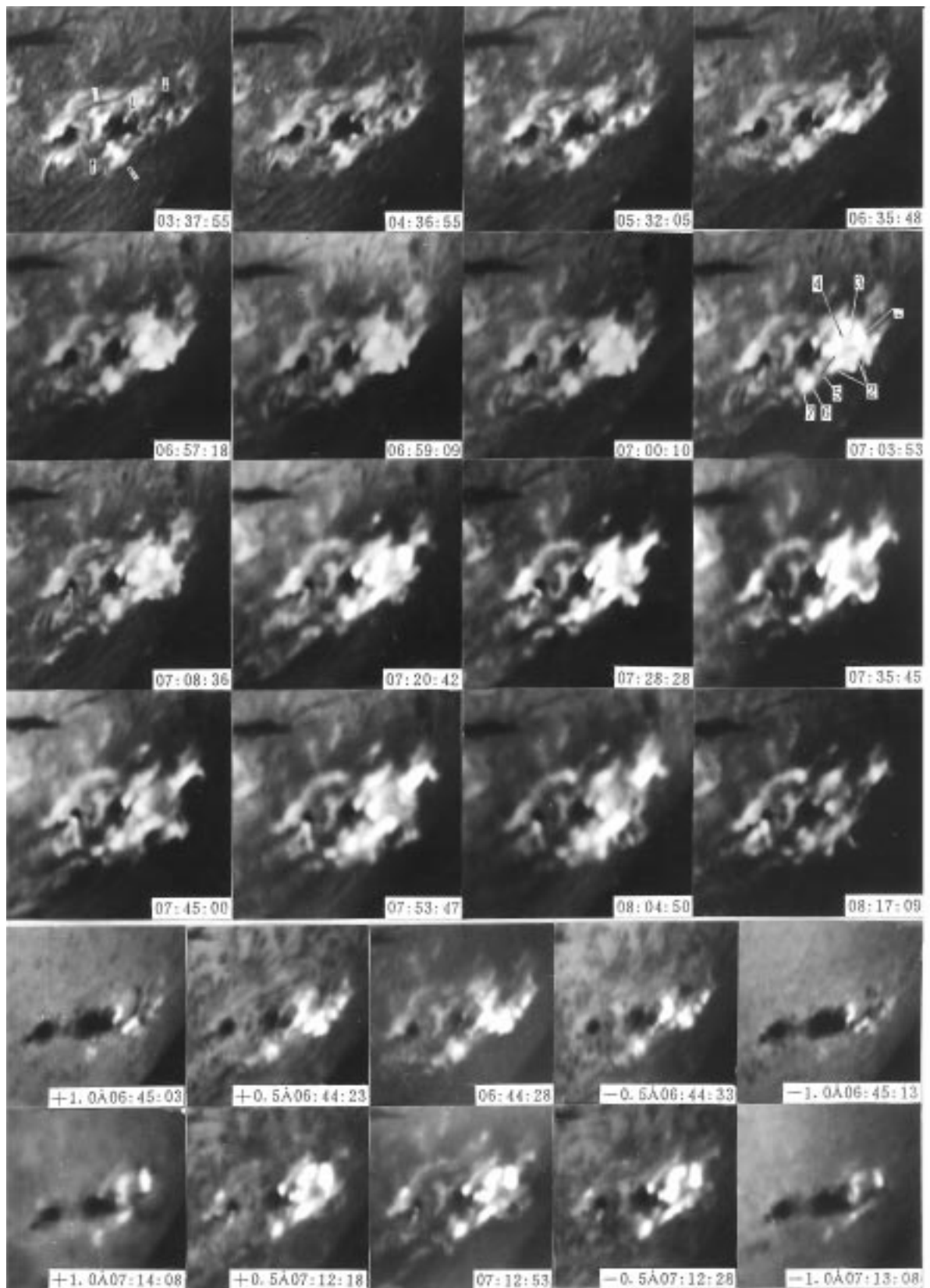


**Fig. 1.** A series of H $\alpha$  filtergrams for the flare on 18 January 1989 in the active region (AR 5312). The arrows indicate active filaments (time in UT). Bottom: H $\alpha$  off-band observations

**Table 3.** Activities in AR 5312

Activity No.	$H_{\alpha}$ evolution (UT)			Imp. or Class		Remarks
	Beg.	Max.	End	$H_{\alpha}$	X-ray	
1	05:08	05:09	05:12D	SF	C9.6	NOAA (1989), YUOBS <sup>a</sup>
2	06:06	06:37	06:37D	SB		NOAA (1989), YUOBS
3	06:40	06:44	06:48	SB		YUOBS
4	07:02	07:07U	07:13D	1F		NOAA (1989), YUOBS
5		07:20			X1.0	NOAA (1989), YUOBS
6		07:28				YUOBS
7		07:35				YUOBS
8		07:45				YUOBS
9		07:53				YUOBS
10	08:05E	08:19U	08:23D	SF		NOAA (1989), YUOBS
11	08:51E	09:12U	09:52	1N	M9.0	NOAA (1989)
12	17:17	17:27	17:46	SF		NOAA (1989)
13	17:57	18:37	19:08	SF		NOAA (1989)

<sup>a</sup> Yunnan Observatory.

**Table 4.** Instruments

Instrument Number	Aperture (mm)	$\phi^*$ (mm)	$A^{**}$ (mm <sup>2</sup> )	Resolution (")	Others
					1
2	400	152	24×16	4.0	Slit height: 20 mm; plane grating: 127×102 mm <sup>2</sup> ; ten bands; average linear dispersion: 1 Å·mm <sup>-1</sup> ; with $H_{\alpha}$ slit jaw monitor; time needed for each scanning: around 1 min.
		420	49×16	1.0	
				1.2( $H_{\alpha}$ )	
3	126	300	36×24	1.0	

\* the diameter of solar image, \*\* the area of frame.

redshift, and then back to blue shift; while the following part (in the east limb) changed from redshift to blue shift and then back to redshift. The motion directions of the leading and following parts are opposite but in the same scale. This seems to be a cycling motion. Kernel 7 shows a redshift. The kernels lying in the umbra and penumbra of the sunspots morphologically showed a small displacement.

### 3.2. Lifetimes of the kernels

It can be seen from Table 3 that several bursts appeared in AR 5312, and 6  $H_{\alpha}$  flare maxima occurred from 07:00 to 08:00UT. Before the first 4 maxima of the  $H_{\alpha}$  flare, the white light flare and its continuum spectra were observed (no observations were made before 07:28UT due to bad weather). In Table 5, it is shown that the kernels of the WLF have different lifetimes, the lifetime of kernel 7 is 5 minutes, kernel 1 is 20 minutes, and for kernels 3, 4, 5 and 6 each is 32 minutes. The lifetime of kernel 2 is over 40 minutes. The phenomenon may indicate that the WLF is typically a long lifetime type. Table 5 also shows that the

WLF appeared 2 to 3 minutes after the  $H_{\alpha}$  flare, and its maxima appeared respectively before the first maximum (such as kernel 7) and 1 to 2 minutes before the second maximum of the  $H_{\alpha}$  flare. However, the disappearance of the WLF is dependent on the lifetimes of the kernels. If the lifetimes of the kernels are shorter, it may disappear faster or vice versa. The kernels all appeared simultaneously, but their maxima and disappearance were in different times. The kernels disappeared before the disappearance of the  $H_{\alpha}$  flare.

### 3.3. The shape and size of the kernels

The kernels have different shapes. Kernels 3, 4 and 7 are nearly circular in shape. Kernels 1, 5 and 6 are elliptical, and kernel 2 is cashew-like. The shapes of the kernels may possibly be dependent on their intrinsic structure and projection on the sight-line direction. The sizes of the kernels are also different, from the observations of the  $H_{\alpha}$  flare at 07:03:53UT, except for kernels 3 and 7. The sizes of other kernels (by the average size of smaller kernels in each kernel) are in the range (1.5 ~ 4)  $10^{17}$  cm<sup>2</sup> (see

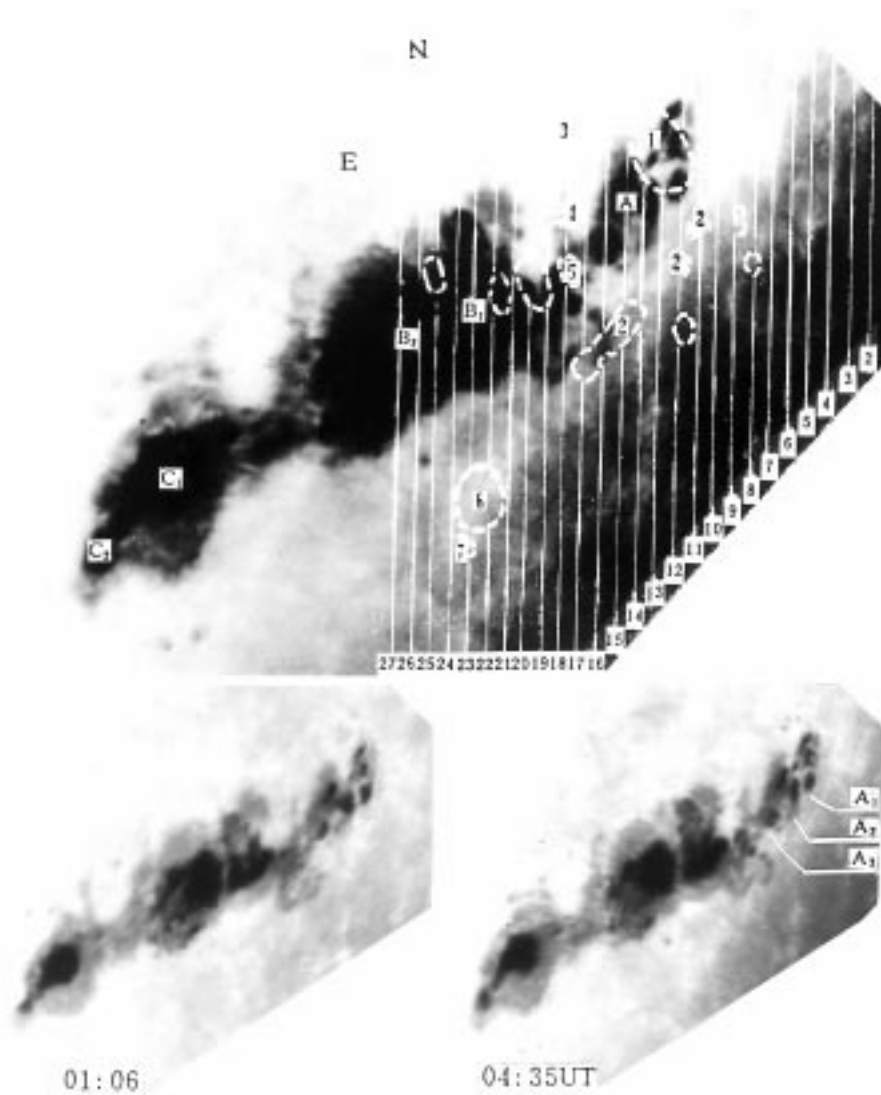


**Fig. 2.** The overlying of photospheric sunspots and chromospheric H $\alpha$ . A, B and C represent sunspot umbra (04:35 UT), the dotted line shows the WLF kernels and solid line with number indicates the spatial location of the incident slit and the scanning step. The bottom of the figure is sunspots on the photosphere before the WLF on 18 January

Table 5). This result is in agreement with those given by Dezso et al. (1980) and Hiei (1980).

### 3.4. Plages

One can see from Figs. 1 and 4 that before the appearance of the WLF there were plages with different area and brightness at the locations of the WLF kernels. The plages were relatively stationary, and some small flares had occurred on them. The lifetimes of the plages seem to be associated with that of the WLF. For example, the lifetime of kernel 7 is short, and that of the plage in its place is also short, only about 20 minutes. The lifetimes of other kernels are longer, and the plages in their places

have longer lifetimes. A typical plage is the one at the place of kernel 6. Its lifetime is about 5 hr.

### 3.5. Fibrils and filaments

Before the flare, chromospheric fibrils bent toward the active region and formed an orderly pattern, nearly in the direction of southeast to northwest, along which the flare and the kernels shifted. It is interesting that the direction along which the chromospheric fibrils moved was just perpendicular to the motion of penumbra fibrils on the photosphere. The phenomenon is in good agreement with the magnetic field observations at Beijing Observatory (Zhang et al. 1991).

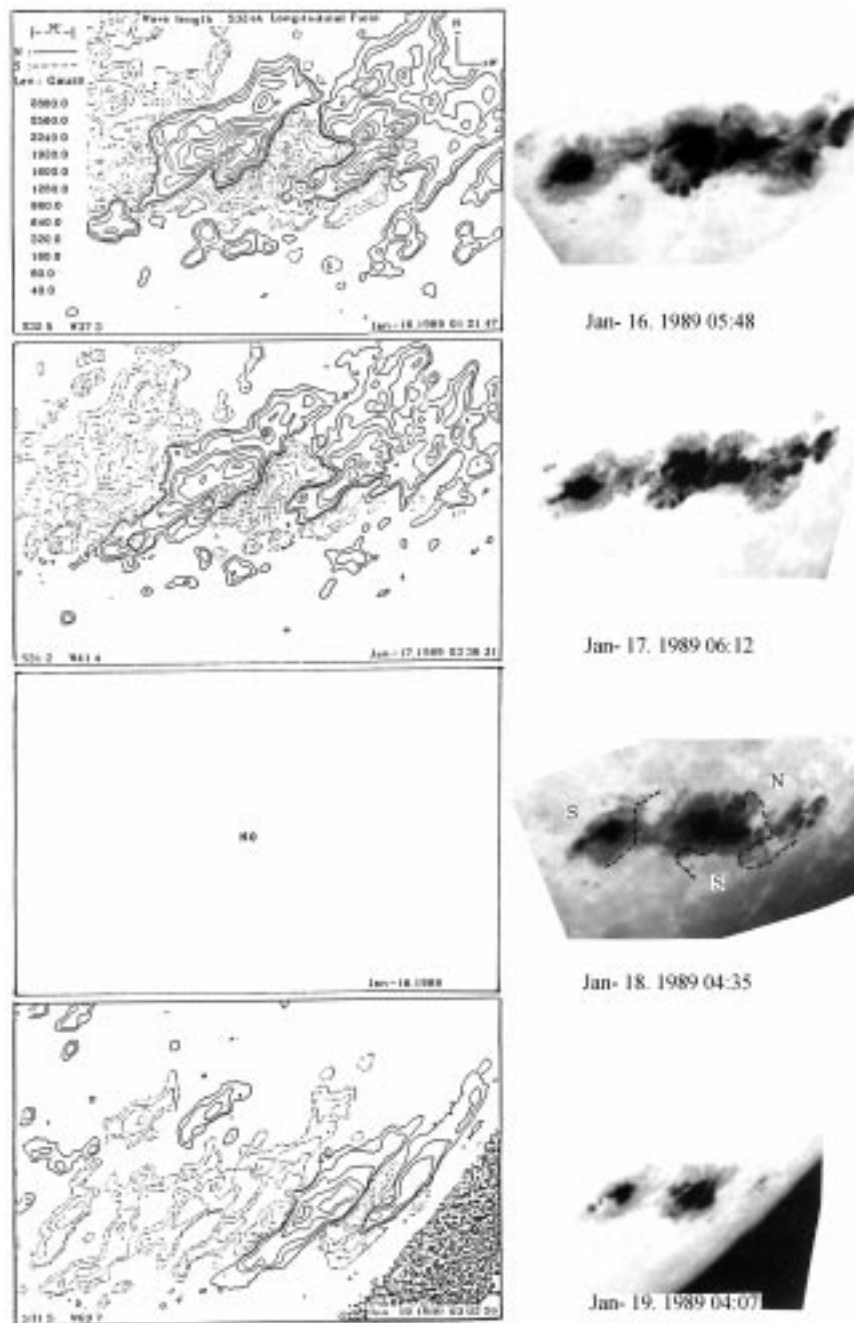


**Fig. 3.** The evolution of sunspots on the photosphere and longitudinal magnetic field (provided by Hairou station of Beijing Observatory)

It also can be seen in Fig. 1 that three branches of a large quiescent dark filament at the west end are activated (i.e. changes take place in the longitudinal components of the magnetic field) before the flare and bend toward the active region, combining with the chromospheric fibrils. In and around the active region, some small filaments (as indicated by the arrow in Fig. 1) are activated one after another before the continuum emission. However, only in the place where the small filaments were activated and

disappeared rapidly (that is, the annihilation of the longitudinal components of the magnetic field) can white light flares and continuum emission be observed. In other areas, only ordinary flares can be observed. For example, no continuum emission was observed in the bright area on the northern end of the light bridge connecting  $B_1$  and  $B_2$ .

**Table 5.** Activities in AR 5312 from 03:37 to 08:17 UT on January 18, 1989

Kernel number	plage	H $_{\alpha}$ activity (UT)				White light flare (UT)				Size $\times 10^{17} \text{cm}^2$	N	
		Beg.	Max.	End	Life	Beg.	SR Time	End	Life			
1	05:32-08:04	06:26	06:37 06:44									
		07:00	07:08 07:20	07:35	00:35	07:03	07:04-07:05 07:19-07:20	07:23	00:20	12	4	
2	05:32-08:17	06:26	06:37 06:44	06:48								
		07:00	07:08 07:20 07:28 07:35 07:45 07:53			07:03	07:04-07:05 07:19-07:20 07:33-07:34 07:43-07:44	07:45	00:42	15	4	
3	06:35-07:53	07:00	07:08 07:20 07:28	07:45	01:00	07:03	07:04-07:05 07:19-07:20			9	a	
4	05:32-07:53	06:26	06:37 06:44	06:48								
		07:00	07:08 07:20 07:28			07:03	07:04-07:05 07:19-07:20			4		
5	06:58-08:04	07:00	07:08 07:20 07:28	07:45	00:45	07:03	07:33-07:34 07:04-07:05 07:19-07:20	07:35	00:32	4		
6	03:37-08:17	06:40	06:44 07:08 07:20 07:28	06:48								
		07:00	07:08 07:20 07:28 07:35	07:45	00:45	07:03	07:33-07:34 07:04-07:05 07:19-07:20	07:35	00:32	5	3	
7	06:52-07:13	07:00	07:08	07:10	00:10	07:03	07:33-07:34 07:04-07:05	07:35	00:32 00:05	b		

a: The internal structure is undistinguishable;  
 b: The size can not be measured precisely;  
 N: Number of smaller kernels;  
 SR Time: Spectral responding time.

### 3.6. Sunspots and magnetic field

AR 5312 passed over the solar disk 3 times in total. The observations were made on its second pass. From its appearance to disappearance on the solar disk, the major sunspot had been surrounded by the same penumbra. The active region showed a complex internal structure and rapid evolution, and new flux emerged continuously. Squeezed and sheared effects also took place between the sunspots. A white light flare (S31 E30, Neidig et al. 1993) occurred on 10 January, and another (S30 W65, see Figs. 1 and 5) appeared on 18 January (Xuan et al. 1991). Before the flare on 18 Jan. there were a number of penumbra fibrils around the spatial locations of all kernels except for kernel 3, i.e. in sunspot group A, between group A and B, and on the light bridge connecting  $B_1$  and  $B_2$ , and some fibrils extended toward the photosphere where some fibrils were in arch-like shape. The initial bright points of the kernels originated in umbra and penumbra, at the bound-

ary between penumbra and the photosphere, in penumbra fibrils, on the photosphere or on the light bridge.

It is shown in Fig. 3 that the magnetic configuration of the active region is a  $\delta$ -structure in the evolution process, and the twisted and closed magnetic neutral lines between the sunspot groups A and B change constantly. On 18 January, the neutral lines were compressed in the east-west direction and began opening from the closed pattern in the south. A large change in the magnetic structure occurred. Kernels 2 and 5 lie on the changing neutral lines and kernels 1, 4, 6 and 7 are near the lines. In the locations of the kernels, new emerging fluxes are enhanced, but the gradient of the longitudinal field is not very large. The magnetic field observations of Beijing Observatory show that the direction of the penumbra fibrils on the photosphere was the same as that of the transversal component of the magnetic field (Zhang et al. 1991). Therefore, the kernels were constrained by the small transverse field on the photosphere.

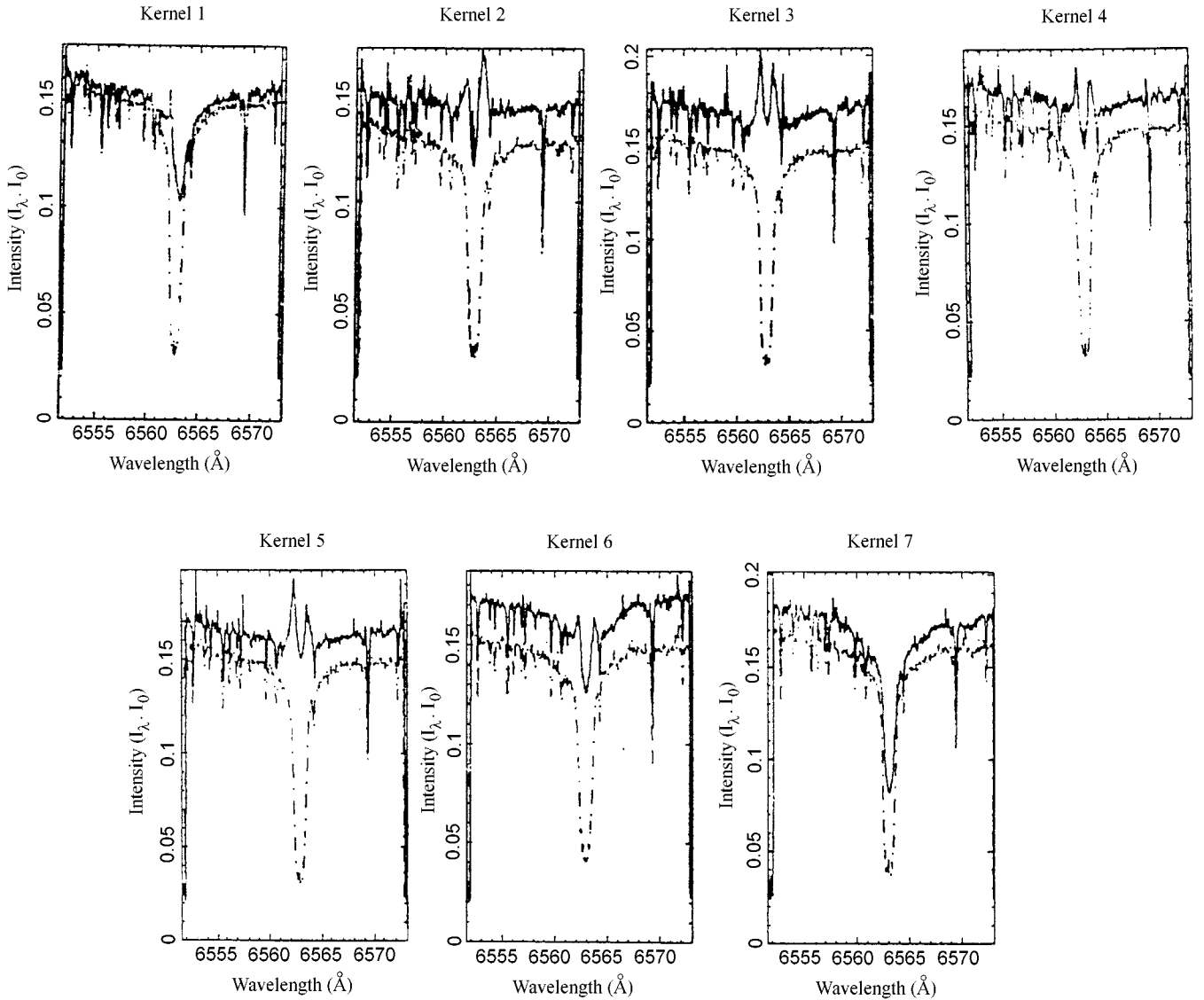


**Fig. 4.**  $H\alpha$  line profile  $[(I_\lambda - I_0) \sim \lambda]$  variations of the kernel 2 in the first time interval. The solid and dotted lines indicate the observed intensity ( $I_\lambda$ ) of the flare and the intensity ( $I_0$ ) of nearby undisturbed background, respectively;  $\lambda$  is wavelength and  $K$  represents the WLF kernels, and the number before  $K$  shows the observing time duration, the first number in the suffix of  $K$  represents kernel number, the second the scanning order, the third and fourth numbers represent the sequential order of line profiles (perpendicular to the slit)

### 3.7. Spectra of the kernels

We present only  $H\alpha$  line profiles of the kernels. The analysis of the other lines can be found in Xuan et al. (1991). It can be seen from Fig. 4 that the spectral line profile centers of the kernels show different changes, and no reversal profile appears at the center of kernel 1. The line profile centers in kernel 2 from intervals 1 to 4 show a strong reversal (see Fig. 4). The closer to the edge of the kernels, the line center reversal is weaker and has no reversal. In the meantime, the line profiles with reversal in kernel 2 have a wide line width, and for others the line width is relatively narrower. The changes in the line width of ker-

nels 3 and 6 and line center reversal are similar to kernel 2. This may suggest that the reversal of the observed line profile centers is not only dependent upon the properties of the kernels themselves, but also has temporal and spatial characteristics. In comparison with Table 2 and from the reversal of the  $H\alpha$  line centers and line width changes, we find that kernels 2, 3 and 6 of the white light flare on 18 January 1989 correspond to the temperature distribution in the semi-empirical models  $F_1$  and  $F_2$  (Machado et al. 1980; Fang et al. 1993), while both line widening and center reversal do not appear in kernel 1. This is possibly due to hydrogen affected by nonthermal excitation and ionization of 100 keV – 1 MkeV ion (Hénoux et al. 1993). It is



shown that the white light flare belongs to a mixed type with properties of both types I and II.

It is also shown in Fig. 4 that the observed profiles of the kernels display different redshift and blue shift. For example, the redshift of the kernel 1 is rather significant. The reversal appears at the centers of the profiles in kernel 3 and the blue end is stronger. At the centers of the profiles in kernel 6, the reversal appears, but the red end is stronger. In the first time interval, kernel 2 shows an obvious blue shift, but at the line profile centers with larger reversal, the red end is stronger. In intervals 2, 3 and 4, the blue end is stronger at the profile centers with an obvious reversal, opposite to the situation in the first interval. This probably indicates that the direction and scale of material motions are different for different kernels in the same white light flare.

#### 4. Conclusions

The optical characteristics of the white light flare on 18 January of 1989 are summarized as the following.

1. Shapes: The WLF consists of 7 kernels in patch-like shape (circular, elliptical or cashew-like form), with sizes from  $1.5 \cdot 10^{17}$  to  $4 \cdot 10^{17}$  cm<sup>2</sup>.

2. Lifetimes: The lifetimes of the WLF kernels vary from several minutes to more than 40 minutes. The kernels appeared simultaneously 2 to 3 minutes after the H $\alpha$  flare, and their maxima occurred before the first maximum (such as kernel 1) and 1 to 2 minutes before the second maximum of the H $\alpha$  flare. They disappeared slowly before the disappearance of the H $\alpha$  flare.

3. Motions: The direction and scale of material motion in the kernels are different.

4. Source points: The initial bright points of the kernels were between umbra and penumbra, in penumbra fibrils, in the area between penumbra fibrils and the photosphere, on the photosphere or on the light bridge.

5. Precursors: There were plages in the locations where the WLF kernels lay, and the plages were relatively stationary. Some small flares had appeared at the sites of the plages, and the lifetimes of the plages are longer than that of the WLF. The chromospheric fibrils near the kernels bent toward the active region, forming an orderly pattern (the development and disappearance of the kernels were basically along this direction). Large chromospheric quiet filaments and small active ones were activated. However, WLFs and their continuum emissions were only observed in places where small filaments were activated and then rapidly disappeared, and some small flares occurred and new flux emerged. In other areas, only ordinary flares were observed.

6. Magnetic field: The magnetic configuration of the photosphere in the active region is in  $\delta$ -structure. The kernels (except for kernel 3) were lying on or near the changing magnetic neutral lines, and the small gradient of

longitudinal field may be constrained by the small transverse field on the photosphere.

7. Class: The central reversal and line width of the spectral line profiles of the WLF kernels exhibit both temporal and spatial properties, and the WLF is of mixed class one with characteristics of both class I and II.

*Acknowledgements.* The authors are thankful to Luan Ti, Wang Hongzhao, Zhang Xiaoyu and other fellows in the spectral research group of Yunnan Observatory for their cooperation in observation. We fully appreciated the help of the PDS group of Purple Mountain Observatory and the Vax computer group of Yunnan Observatory in our data processing. We should also be obliged to Huairou station of BeiJing Observatory for providing the magnetic field data. This work was supported by the grant 94A087M of the Science Foundation of Yunnan Province and the work of XMG and JL were also partly supported by the grants 19333041 and 19333042, respectively, of the National Scientific Foundation of China.

#### References

- Ai G.X., Hu Y.F., 1986, Publ. Beijing Astron. Obs. 8, 1
- Dezső L., Gesztelyi L., Kondás L., et al., 1980, Solar Phys. 67, 317
- Fang C., Ding M.D., 1994, Progress Astron. 12, 100
- Fang C., Hénoux J.C., Gan W.Q., 1993, A&A 274, 917
- Hénoux J.C., Fang C., Gan W.Q., 1993, A&A 274, 923
- Hiei E., 1980, Solar Phys. 80, 113
- Huang Y.R., Yin S.Y., Fang C., 1991, Acta Astron. Sinica 32, 421
- Machado M.E., Avrett E.H., Falciant R., et al., 1986, in Neidig D.F. (ed.) The Lower Atmosphere of Solar Flares, Proceedings of NSO/SMM Symposium, Sunspot, 1985, NSO, 483
- Machado M.E., Avrett E.H., Vernazza J.E., Noyes R.M., 1980, ApJ 242, 336
- Neidig D.F., 1989, Solar Phys. 121, 261
- Neidig D.F., Cliver E.W., 1983a, AFGL-TR-38-0257
- Neidig D.F., Wiborg P.H., Gillam L.B., 1993, Solar Phys. 144, 169
- NOAA, 1989, SGD Prompt Reports, 534(1), 34
- Sakurai T., Ichimoto K., Hiei E., et al., 1992, Astron. Soc. Japan 44, L7
- Schmieder B., Hahyard M.J., Ai G.X., et al., 1994, Solar Phys. 150, 199
- Sotirovski P., Boyer R., Hiei E., Vince I., 1992, A&A 262, 597
- Wu M.C., Li Z.K., Li Z., et al., 1990, Pub. Yunnan Obs. 3, 1
- Xuan J.Y., Lin J., 1993, Solar Phys. 144, 307
- Xuan J.Y., Lin J., Zhong S.H., et al., 1991, in Schmieder B. and Priest E.R. (eds.) Flares 22 Workshop "Dynamics of Solar Flares", Chantilly, France 1990, Observatoire de Paris, DASOP, p. 157
- Zhang H.Q., Ai G.X., Sakurai T., Kurokawa H., 1991, Solar Phys. 136, 269
- Zhu C.L., Shen L.X., 1992, Acta Astrophys. Sinica 12, 374